

Sussex Research

Precipitation, cloud cover and Forbush decreases in galactic cosmic rays

Dominic Kniveton

Publication date

01-09-2004

Licence

This work is made available under the **Copyright not evaluated** licence and should only be used in accordance with that licence. For more information on the specific terms, consult the repository record for this item.

Citation for this work (American Psychological Association 7th edition)

Kniveton, D. (2004). *Precipitation, cloud cover and Forbush decreases in galactic cosmic rays* (Version 1). University of Sussex. <https://hdl.handle.net/10779/uos.23312768.v1>

Published in

Journal of Atmospheric and Terrestrial Physics

Link to external publisher version

<https://doi.org/10.1016/j.jastp.2004.05.010>

Copyright and reuse:

This work was downloaded from Sussex Research Open (SRO). This document is made available in line with publisher policy and may differ from the published version. Please cite the published version where possible. Copyright and all moral rights to the version of the paper presented here belong to the individual author(s) and/or other copyright owners unless otherwise stated. For more information on this work, SRO or to report an issue, you can contact the repository administrators at sro@sussex.ac.uk. Discover more of the University's research at <https://sussex.figshare.com/>

Precipitation, cloud cover and Forbush decreases in galactic cosmic rays

Article (Unspecified)

Citation:

Kniveton, Dominic R (2004) Precipitation, cloud cover and Forbush decreases in galactic cosmic rays. *Journal of Atmospheric and Terrestrial Physics*, 66 (13-14). pp. 1135-1142. ISSN 1364-6826

This version is available from Sussex Research Online: <http://sro.sussex.ac.uk/1691/>

This document is made available in accordance with publisher policies and may differ from the published version or from the version of record. If you wish to cite this item you are advised to consult the publisher's version. Please see the URL above for details on accessing the published version.

Copyright and reuse:

Sussex Research Online is a digital repository of the research output of the University.

Copyright and all moral rights to the version of the paper presented here belong to the individual author(s) and/or other copyright owners. To the extent reasonable and practicable, the material made available in SRO has been checked for eligibility before being made available.

Copies of full text items generally can be reproduced, displayed or performed and given to third parties in any format or medium for personal research or study, educational, or not-for-profit purposes without prior permission or charge, provided that the authors, title and full bibliographic details are credited, a hyperlink and/or URL is given for the original metadata page and the content is not changed in any way.

Precipitation, cloud cover and Forbush decreases in galactic cosmic rays

Dominic R. Kniveton¹

Journal of Atmosphere and Solar-Terrestrial Physics

¹School of Chemistry, Physics and Environmental Science, University of Sussex, Falmer,
Brighton, BN1 9QJ, UK

d.r.kniveton@sussex.ac.uk

Tel: +44 1273 877757

Fax: +44 1273 677196

Formatted

Keywords: Cosmic rays, clouds, precipitation, climate, ISCCP, Forbush decrease, solar variability

Abstract

The results of a study to explore variations in cloud cover, over regions that are minimally affected by rainfall and heavy rainfall, and that are coincident with variations in the galactic cosmic ray flux, are presented. Using an extensive record of global satellite derived cloud and rainfall products from the International Satellite Cloud Climatology Project (ISCCP) D1 data series and Xie and Arkin (1996), epoch superposition analysis of a sample of events of short term decreases in the galactic cosmic ray flux, is conducted. Analysis of data that is largely free from the influence of rainfall and heavy rainfall, averaged over 10-degree geomagnetic latitude (ϕ) bands reveals that cloud cover is reduced at high latitudes, and at middle and lower (including equatorial) latitudes over regions of relatively higher cloud cover, over both land and ocean surfaces, while increasing over ocean surfaces at middle and lower latitudes in regions of thinner cloud.

Introduction

Three possible mechanisms have been proposed to explain the coupling between solar activity and terrestrial climate; variations in the total irradiance; variations in the spectral irradiance in the ultraviolet portion of the electromagnetic spectrum; and variations in the solar wind and the flux of energetic particles [Reid 2000]. Of these the last mechanism has proved particularly controversial especially after the studies of Svensmark and Fris-Christensen (1997) and Marsh and Svensmark (2000) in which variations in galactic cosmic rays (GCR) were related to changes in cloudiness and proposed as being responsible for a radiative forcing of 1.4 Wm^{-2} over the period 1901-1995.

A number of reassessments of the work of Svensmark and Friis-Christensen (1997), and Marsh and Svensmark (2000), by Kernthaler et al. (1999), Farrar (2000), Jorgensen and Hansen (2000), Kristijansson and Kristiansen (2000) and Sun and Bradley (2002), have been undertaken. These studies have raised doubts about the longer-term stability of the cloud-GCR relationship and suggested that the observed variability in cloud cover may be related to the internal climate mechanisms of El Nino-Southern Oscillation and volcanic activity rather than GCR variability. Instead of examining changes in cloud cover over interannual timescales Todd and Kniveton (2001) choose to focus their research into the effect on cloud of short-term Forbush decreases in GCR. The advantage of this is that there is no known natural internal modes of climate variability that operate with similar temporal characteristics as Forbush decrease events. Their study found a small but significant decline in the global proportion of cloud cover of up to 1.4% immediately prior and following Forbush decrease events (Todd and Kniveton, 2001].

It is notable that the results of Todd and Kniveton (2001) showed very little similarity with the cloud cover changes at interannual time scales observed (and ascribed to GCR variability) by Svensmark and Friis-Christensen (1997), and Marsh and Svensmark (2000). In those studies, positive correlations between interannual cloud cover and GCR were strongest for low-level cloud (on average 2km) and over ocean surfaces of the tropics and midlatitudes. By contrast Todd and Kniveton (2001) found no significant anomalies in low-level cloudiness associated with short term GCR variability, instead the anomalies on the whole being concentrated at high latitudes. Physical explanations for a link between galactic cosmic rays and cloudiness have been based around cosmic ray

ionisation related direct and indirect impacts on cloud microphysics. The direct influence on cloud includes ion-mediated nucleation, while indirect mechanisms include the impact of GCR ionisation on atmospheric electrical conductivity within the Global Electric Circuit and the subsequent effect on electro-scavenging (Carslaw et al, 2003).

Cloud cover is not the only atmospheric parameter that has been linked to changes in galactic cosmic ray. A study of precipitation and precipitation efficiency and GCR at high geomagnetic latitudes by Kniveton and Todd (2001) revealed a strong correlation at interannual timescales. Clearly precipitation and cloud processes are closely linked with each other. While obviously without cloud there is unlikely to be precipitation, precipitation ultimately reduces cloud cover through the removal of cloud water. This latter process may result in some of the cloud cover changes, which are related to variability in cosmic rays, being negated by changes in precipitation and a dampening of the observable response of the cloud. It is therefore the aim of this study to explore cloud cover changes coincident with changes in GCR, excluding locations where there is rainfall and excluding locations where there is heavy rainfall. In particular the analysis will be carried out using geomagnetic latitude bands to reduce the influence of meteorological noise. The reason for concentrating on the geomagnetic latitudinal response of cloud cover is that there is a geomagnetic latitude variation in GCR.

Method

The International Satellite Cloud Climatology Program (ISCCP) produces the currently most comprehensive database of global cloud cover. A range of cloud parameters is

available from ISCCP, for the period 1986 to 1994, for every 3 hours on a 2.5° latitude-longitude grid (Rossow et al., 1996). For this study I have simply concentrated on one variable of this dataset; the proportion of all pixels defined as cloudy. No attempt is made to separate the cloud types into liquid and ice cloud due to the observation by Todd and Kniveton (2001) that no significant cloud anomalies during Forbush decreases were observed where the ISCCP data involved daytime observations, and the need for visible wavelength measurements to make the distinction between ice and liquid clouds. The methodology used in this study is the ‘epoch superposition’ analysis, as used in previous studies of this kind. The method relies on selecting a sample of key dates and extracting ISCCP D1 data for the period 5 days prior to 5 days following each date. The cloud parameters are then averaged over the sample for each time slot (day -5 to day 5) separately. This is akin to compositing routinely used in climate analysis. The difference between conditions prior to, during and after FD events (key date) can then be established by subtracting the mean values at different time slots. Here, I define a ‘base period’ sample representative of conditions prior to an event as the mean of days -5 to -3 . The mean cloud values at all days from day -2 to day 5 are then derived and from this the anomaly is obtained by subtracting the mean of the base period. The result is tested for local statistical significance using a t-test at the 0.05 probability level. Throughout, the anomalies are given as absolute values rather than as a percentage of the base period value.

In this study I have selected a sample of isolated FD events (separated by more than 11 days from another event). These dates represent the onset of FD events (defined by a

decline greater than 3%) at the earth's surface as recorded by the neutron monitor at Mount Washington, USA (44.3N, 288.7E). Over the relatively short period for which we have ISCCP data there are total of 50 FD events. Some of these coincide (within 3-days either side) with solar proton (SP) events. It has been hypothesized that during FD events associated with SP events an increase in ionization (and any effect on cloud) from solar protons is likely to oppose any decrease associated with a decline in GCR. To isolate the GCR signal from that of SP I have selected the FD events into separate samples of 23 FD events when no SP event occurs (hereafter referred to simply as FD events) (see Todd and Kniveton, 2001, for a list of the dates).

Rainfall has a characteristically high spatial and temporal variability. This makes its measurement either by in-situ, e.g. rain gauges, and remote methods, e.g. satellite data, difficult. Presently, satellite based retrievals of global rainfall for extended periods, are mainly limited to estimates at monthly timescales. In this study in order to delineate regions of rainfall I use the Climate Prediction Center Merged Analysis of Precipitation (CMAP) product. This is derived from a weighted combination of rainfall estimates from satellite infrared and passive microwave data, numerical weather prediction model analyses and surface based precipitation observations, and provides a record of global rainfall estimates, on a 2.5° grid from 1979 to present (Xie and Arkin, 1996). To develop a mask for filtering the cloud data to remove all possible rainfall effects, the months for which there were Forbush decrease events were selected and a climatology of average monthly rainfall derived. When using large-scale (and large grid cell) data the distinction between rain and no rain can be considered a fuzzy concept with some areas within in a

grid cell of low rainfall not raining and other areas raining. Thus when removing areas where the grid cell has a rainfall above 0mm/d would exclude a large number of areas over which there was no rainfall and considerably reduce the area available for the analysis of changes in cloud cover. Therefore it was decided to choose a rainfall threshold minimally larger than 0mm/d to isolate yet observe changes in rain free clouds. Additionally it was decided to choose a higher rain rate threshold to remove solely heavily precipitating clouds. Thus the thresholds of 1mm/d and 5mm/d were selected to screen out those grid cells where rainfall in any of the dates was above and equal to these thresholds. Lastly the grid cells were averaged along 10° geomagnetic latitude (ϕ) bands for analysis of significant changes (as described above). The decision to average the data in 10° bands was taken to reduce the noise from the inevitable day-to-day meteorological processes.

Results

Figure 1 shows the mean proportion of cloud cover during the ‘base period’ day -5 to day -3 for the FD events. The structure of cloud cover is in very close agreement both in terms of absolute and relative cloud amounts with the long-term average cloud conditions determined from the ISCCP D2 dataset (Rossow and Schiffer, 1999). From this I am confident that our sample of events is representative of the long-term climatology, providing evidence that our sample size is large enough to highlight any systematic changes in cloud cover associated with FD events.

In Figure 2a the changes of cloud cover at 10° geomagnetic latitudes are shown for all the FD events over land and ocean surfaces, without any masking for raining locations. Significant anomalies (at the 0.05 probability level) emerge only in particular locations, dominated by large negative anomalies (up to 12.6%) over the polar latitudes of the southern hemisphere (poleward of $\varphi=70^\circ\text{S}$) throughout the FD epoch, peaking at day 1. There are smaller negative anomalies (5.7%) over the polar latitudes of the northern hemisphere (poleward of $\varphi=80^\circ\text{N}$) significant only on day 0, and small positive anomalies (2.1%) from $\varphi=20^\circ\text{--}30^\circ\text{N}$, significant on days 2, 4 and 5. In Figures 2b and 2c these changes are shown but separated according to whether they were for locations over land or sea. Over land in addition to the decreases at the poles there is a small significant positive anomaly (3.4%) on day 2 at $\varphi=0^\circ\text{--}10^\circ\text{N}$, but no positive anomaly at $\varphi=20^\circ\text{--}30^\circ\text{N}$. Over ocean the negative anomalies are still present at the higher latitudes, however there are now additional negative anomalies at $\varphi=10^\circ\text{--}20^\circ\text{S}$ and $30^\circ\text{--}40^\circ\text{S}$ of 2.3% and 1.3%. The positive anomaly at $\varphi=30^\circ\text{--}40^\circ\text{N}$ in Figure 2a is also present in Figure 2c (2.7%).

When the 1mm/d rain mask is applied the amount of cloud cover used to calculate the geomagnetic latitude bands is reduced considerably (Figure 3). The changes of cloud cover for all the FD events over land and sea surfaces, where there is less than 1mm/d rainfall, are shown in Figure 4a. The significant negative anomalies over polar latitudes are still present as there is little influence of the rain mask at these locations. However we now see a significant negative anomaly peaking the day after the key date at $\varphi=0^\circ\text{--}10^\circ\text{S}$ of 4.5%, and a significant positive anomaly at $\varphi=50^\circ\text{--}60^\circ\text{S}$ again peaking the day after the key date with a magnitude 3.4%. When these anomalies are separated according to

whether they occur over land or sea (Figures 4b and 4c), over land there is a significant negative anomaly two days after the key event at $\phi=0-10N$ of 8.5% in addition to the negative anomalies (peaking at 7.2% and 12.6%) at the northern and southern polar latitudes. While over the sea a significant negative anomaly of 4.8% occurs at $\phi=0-10S$ and a significant positive anomaly at 3.5% at $\phi=50-60S$.

The 5mm/d mask allows more locations to be considered in the geomagnetic latitude band averages (Figure 5). Over all surfaces we see significant negative anomalies at $\phi=0-10S$, 80-90N, 70-80S and 80-90S of 3.3%, 5.7%, 4.8% and 12.6% respectively (Figure 6a). The breakdown of these results according to surface type (Figures 6b and 6c) reveals statistically negative anomalies over the oceans at $\phi=80-90N$, 40-50S, and 70-80S of 7%, 1.3% and 4.7% on the key date, one day after the key date and peaking two days after the key date, respectively. Significant positive anomalies are found at $\phi=20-30N$, and 10-20S on the key date and three days after the key date of 2.7% and 2.5% respectively. Over land all the significant anomalies are decreases of cloud cover of peaking at 12.6%, 7.1% and 5.1% at $\phi=70-90S$, 80-90N and 0-10N on the day after the key date, the key date and two days after the key date, respectively.

Discussion and conclusion

In this study I have explored the changes in clouds that are unlikely to be raining or heavily raining coincident with daily decreases (known as Forbush decreases) in the galactic cosmic ray flux. Analysis of the precipitation and heavy precipitation ‘free’ cloud cover changes for all surfaces using 10° geomagnetic latitude band averages reveals

a more varied pattern of change than revealed with an analysis of all cloud. In particular it is observed that statistically significant reductions in cloud cover are observed at both high and equatorial latitudes both over land and sea surfaces when cloud areas are limited to those likely to be precipitation free. When limiting the analysis to those regions free of heavy precipitation statistically significant reductions in cloud cover are additionally observed at middle latitudes. However statistically positive anomalies also appear at $\phi=20-30\text{N}$, and $10-20\text{S}$ over oceans. Thus it appears that over regions where there is thicker cloud cover, the cloud cover is significantly reduced during Forbush decreases of galactic cosmic rays, whereas over ocean regions where there is thinner cloud cover, the cloud cover is increased. These observations may go some way to explain the discrepancies between the observed changes by (Marsh and Svensmark 2000; Todd and Kniveton 2001) in cloud cover at interannual and daily timescales.

Lastly various caveats needed to be added for consideration of the results presented. Firstly, it must be remembered that these conclusions are based on a small sample of events. Secondly it is possible that the satellite instruments that supply the data, and/or the algorithms used to extract cloud information, are not sufficiently sensitive or accurate, respectively, such that data errors are large relative to any cloud signal. As such it may be considered that the observed anomalies are merely spurious. However the symmetry of the anomalies in both hemispheres suggest otherwise.

Acknowledgements

The author would like to thank the International Satellite Cloud Climatology Program (ISCCP) and the Goddard Institute for Space Studies for production of the ISCCP data and the Distributed Active Archive Center at Langley Research Center, EOSDIS, for its distribution. These activities are sponsored by NASA's Mission to Planet Earth. I am also grateful to the NOAA National Geophysical Data Center for data on Forbush decreases in Cosmic Ray flux. Hourly neutron monitor data was obtained from the Space Physics Data System of the University of Chicago (funded by National Science Foundation Grant ATM-9912341). The author would also like to thank Prof. Brian Tinsley for his useful comments on preparing this article.

Figure captions

Figure 1. Mean total cloud proportion during the ‘base period’ for all Forbush decrease events (days –5 to –3 prior to onset of FD events).

Figure 2 a, b, c. Zonal mean (averaged over 10 degree geomagnetic latitude bands) total cloud proportion anomalies (relative to base period) for days –1 to 5, for (a) all FD events, (b) all FD events over land surfaces, and (c) all FD events over sea surfaces. Positive (negative) anomalies have solid (dotted) contours. The contour interval is 1% and statistically significant anomalies (at 0.05 probability level) are shaded.

Figure 3. Mean total cloud proportion during the ‘base period’ for all Forbush decrease events (days –5 to –3 prior to onset of FD events), excluding those grid cells where the average monthly rainfall for the sampling period is greater or equal to 1mm/d. White denotes rain mask.

Figure 4 a, b, c. Zonal mean (averaged over 10 degree geomagnetic latitude bands) total cloud proportion anomalies (relative to base period), for days –1 to 5, for (a) all FD events, (b) all FD events over land surfaces, and (c) all FD events over sea surfaces, excluding those grid cells where the average monthly rainfall for the sampling period is greater or equal to 1mm/d. Positive (negative) anomalies have solid (dotted) contours. The contour interval is 1% and statistically significant anomalies (at 0.05 probability level) are shaded.

Figure 5. Mean total cloud proportion during the ‘base period’ for all Forbush decrease events (days –5 to –3 prior to onset of FD events), excluding those grid cells where the average monthly rainfall for the sampling period is greater or equal to 5mm/d. White denotes rain mask.

Figure 6 a, b, c. Zonal mean (averaged over 10 degree geomagnetic latitude bands) total cloud proportion anomalies (relative to base period) for days -1 to 5 , for (a) all FD events, (b) all FD events over land surfaces, and (c) all FD events over sea surfaces, excluding those grid cells where the average monthly rainfall for the sampling period is greater or equal to 5mm/d . Positive (negative) anomalies have solid (dotted) contours. The contour interval is 1% and statistically significant anomalies (at 0.05 probability level) are shaded.

References

- Carslaw K.S., R.G. Harrison and J. Kirkby, 2003. Cosmic rays, clouds and climate, *Science*, 298, 5599, 1732-1737.
- Farrar P.D., 2000. Are cosmic rays influencing oceanic cloud coverage-or is it only El Nino? *Climatic Change*, 47 (1-2): 7-15.
- Jorgensen T.S., and Hansen, A.W., 2000. Comments on "Variation of cosmic ray flux and global cloud coverage - a missing link in solar-climate relationships" by Henrik Svensmark and Eigil Friis-Christensen [Journal of Atmospheric and Solar-Terrestrial Physics 59 (1997) 1225-1232], *J. Atmos. & Solar Terr. Phys.*, 62, 73-77.
- Kernthaler S.C., Toumi R., and Haigh, J., 1999. Some doubts concerning a link between cosmic ray fluxes and global cloudiness, *Geophys. Res., Lett.*, 26, 863-865.
- Kniveton, D.R., and Todd, M.C., 2001: On the relationship of cosmic ray flux and precipitation. *Geophysical Research Letters*, 28 (8): 1527-1530.
- Kristjansson J. E., and Kristiansen, 2000. Is there a cosmic ray signal in recent variations in global cloudiness and cloud radiative forcing, *J. Geophys. Res.*, 105, 11851-11863.
- Marsh, N. and Svensmark, H., 2000. Low cloud properties influenced by cosmic rays, *Phys. Rev. Lett*, 85, 5004-5007.
- Rossow, W. B., Walker, A.W., Beuschel, D.E., and Roiter, M.D., 1996. ISCCP documentation of new cloud datasets. WMO Tech. Document 737, 115pp, World Climate Research Program, Geneva, Switzerland.
- Sun, B.M., and Bradley, R.S., 2002. Solar influences on cosmic rays and cloud formation: A reassessment. *Journal of Geophysical Research*, 107 (D14): art. no. 4211.

Svensmark, H., and Friis-Christensen, E., 1997. Variation of cosmic ray flux and global cloud coverage – A missing link in solar-climate relationships, *J. Atmos. & Solar Terr. Phys.*, 59 1225-1232.

Todd, M.C. and Kniveton, D.R., 2001: Changes in cloud cover associated with Forbush decreases of galactic cosmic rays. *Journal of Geophysical Research*, 106 (D23): 32031-32041 .

Xie P. P. and Arkin, P.A., 1996. Analyses of global monthly precipitation using gauge observations, satellite estimates, and numerical model predictions. *J. Climate*, 9, 840-858.

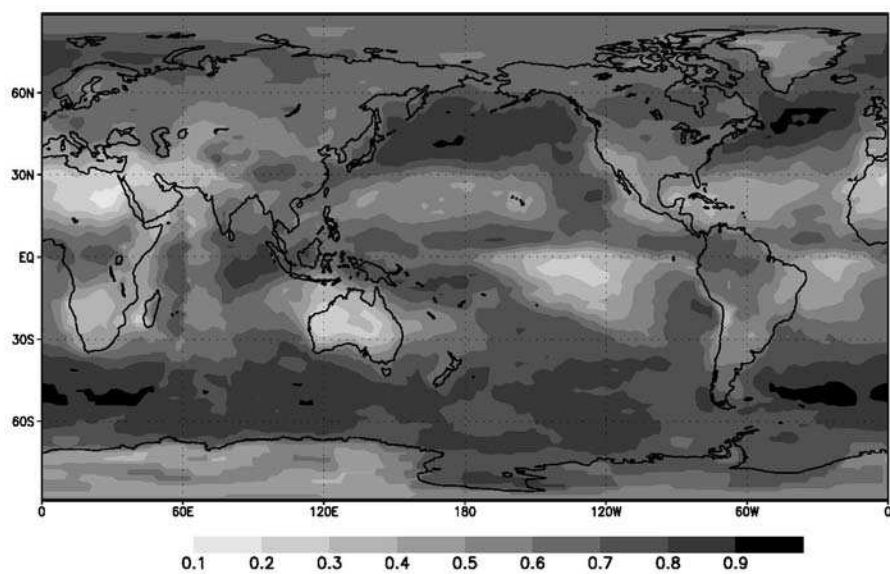


Figure 1.

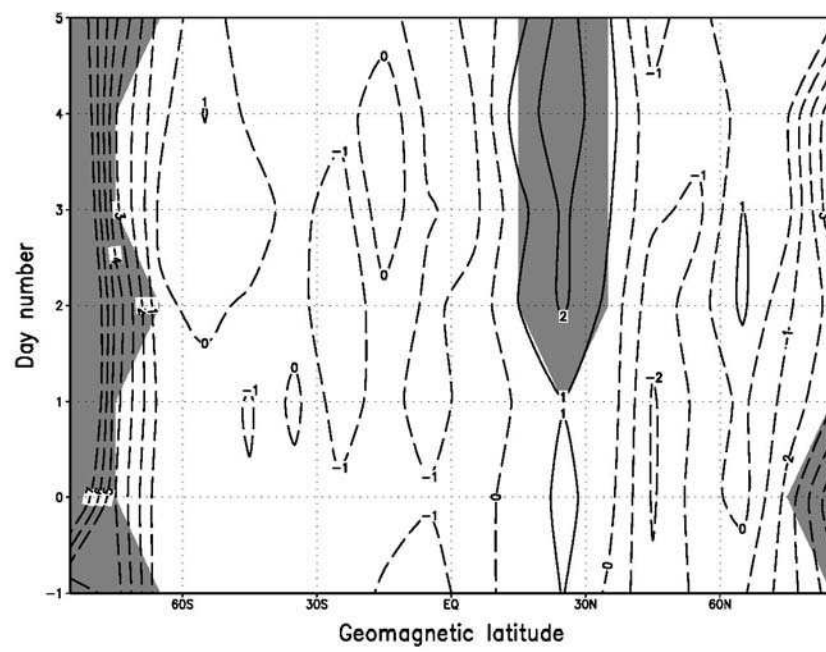


Figure 2a

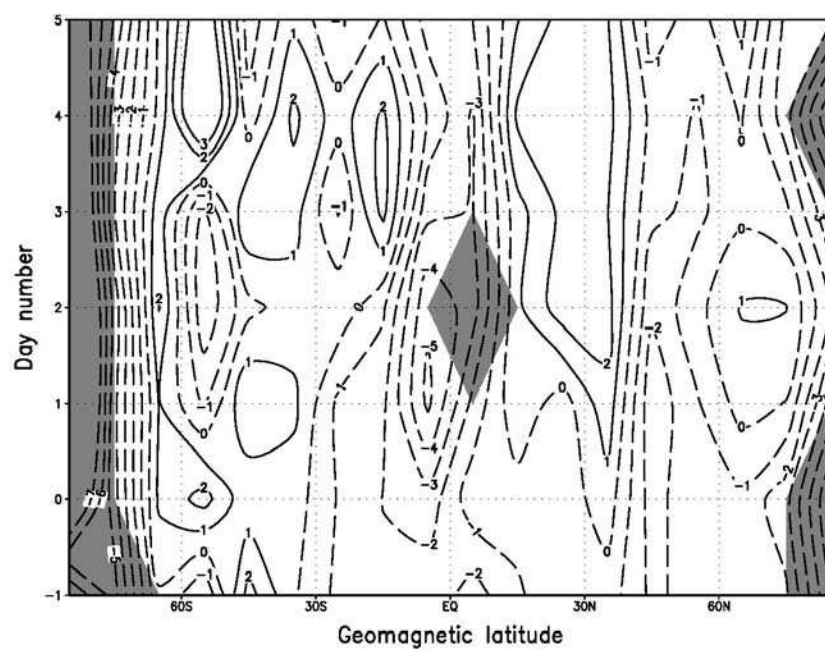


Figure 2b.

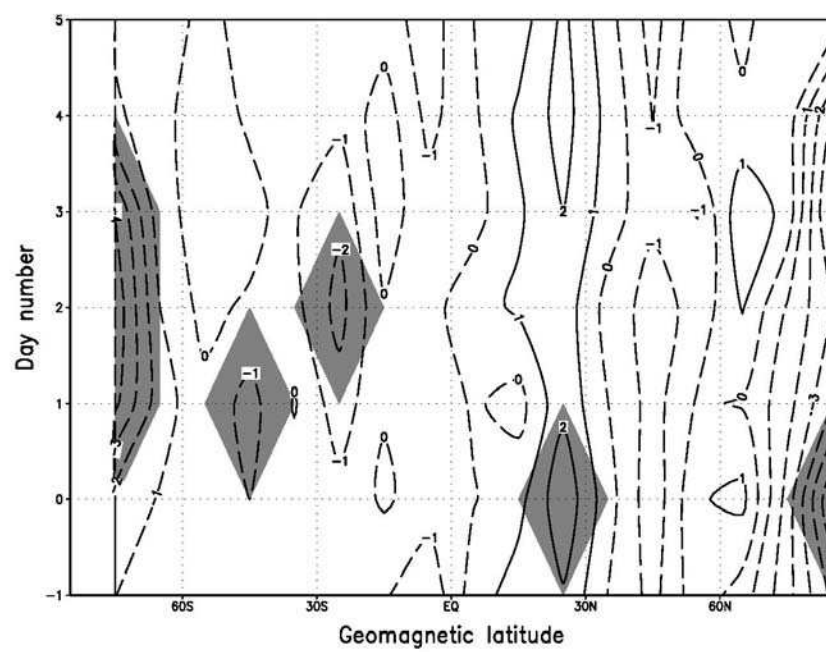


Figure 2c.

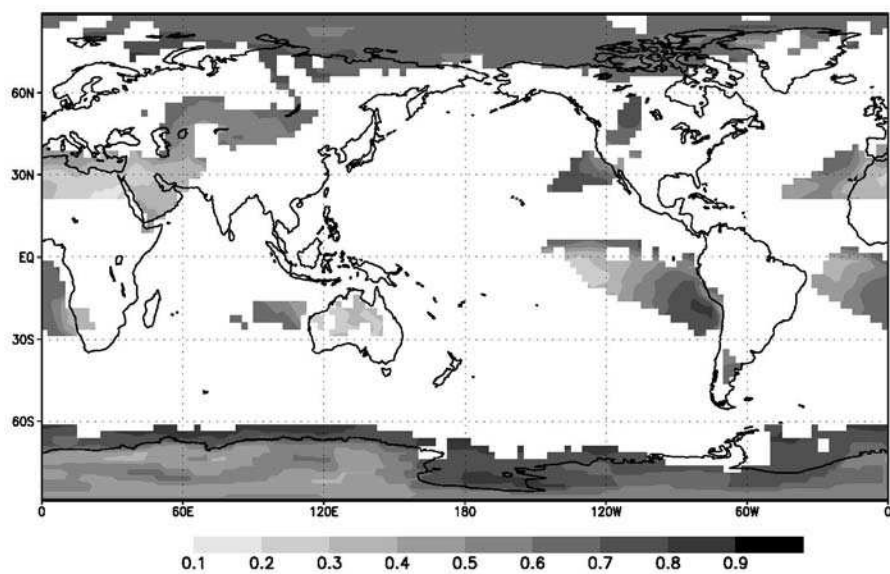


Figure 3.

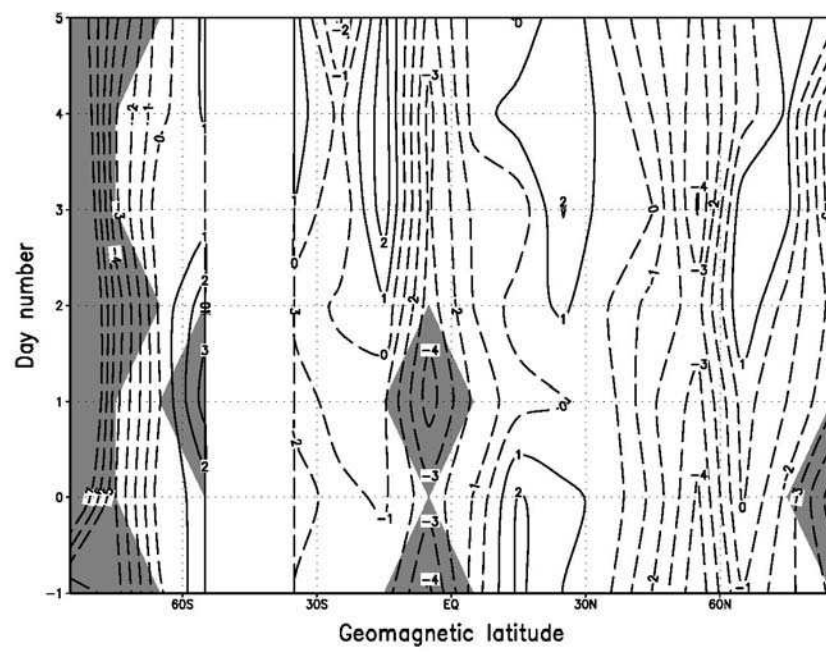


Figure 4a.

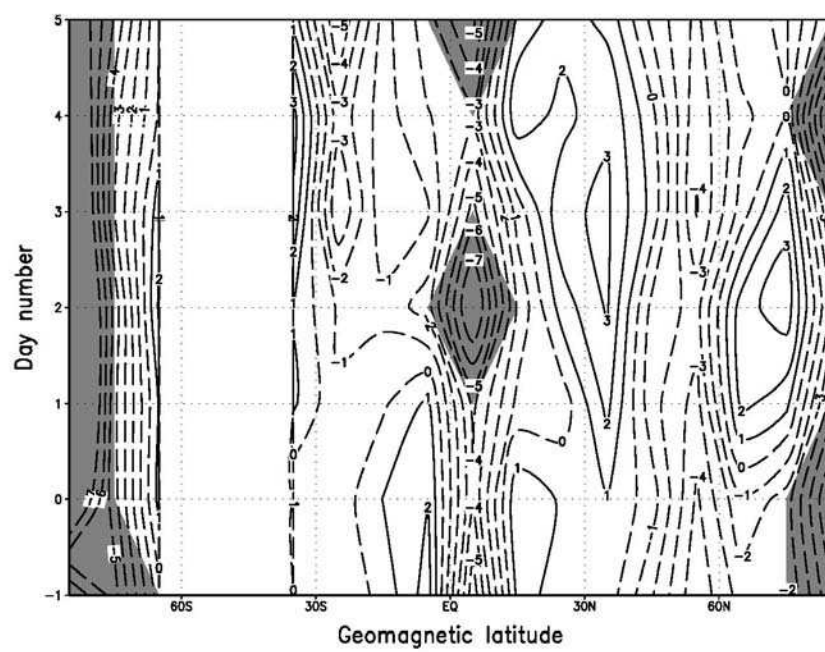


Figure 4b.

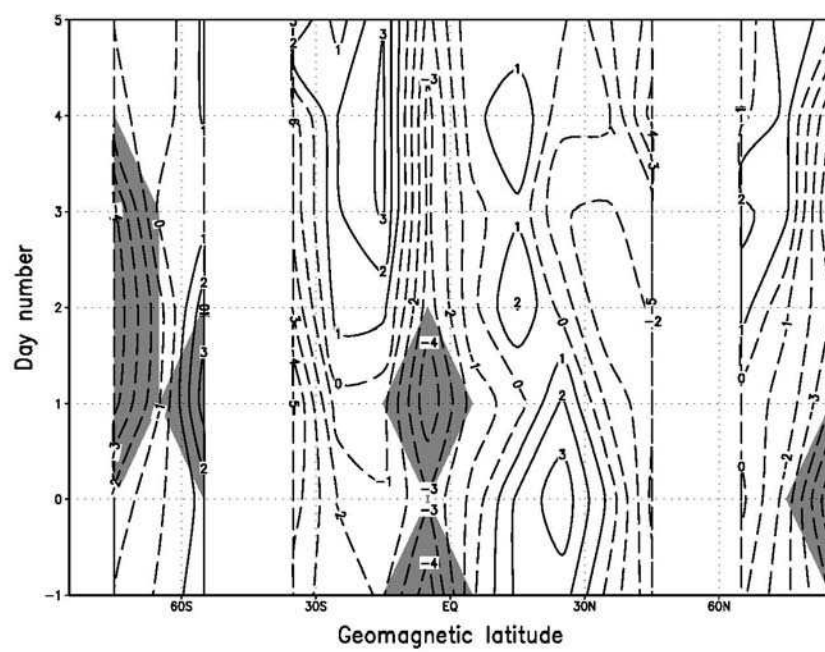


Figure 4c.

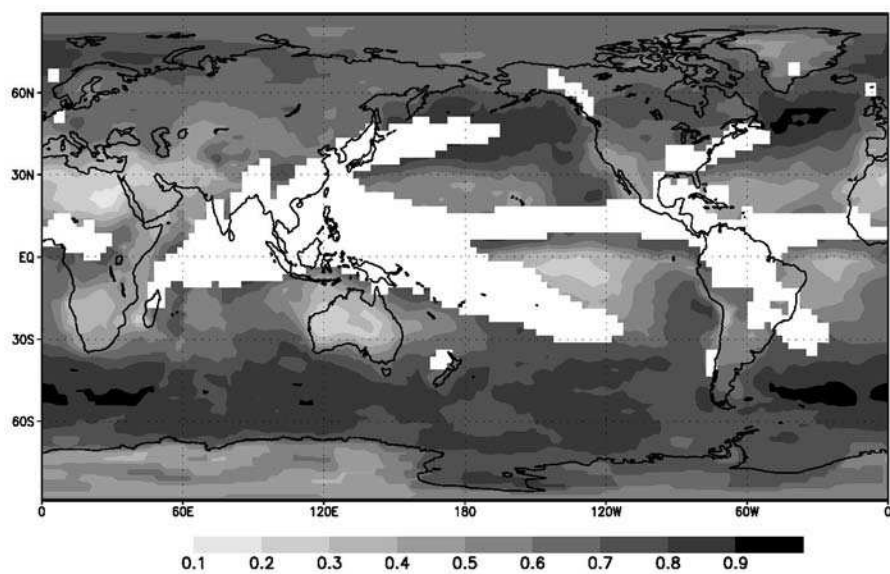


Figure 5.

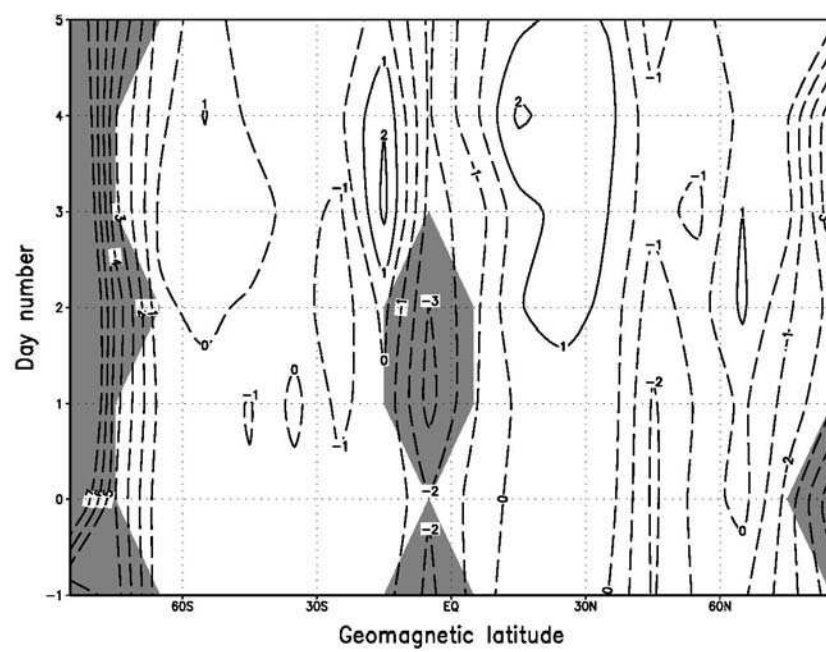


Figure 6a.

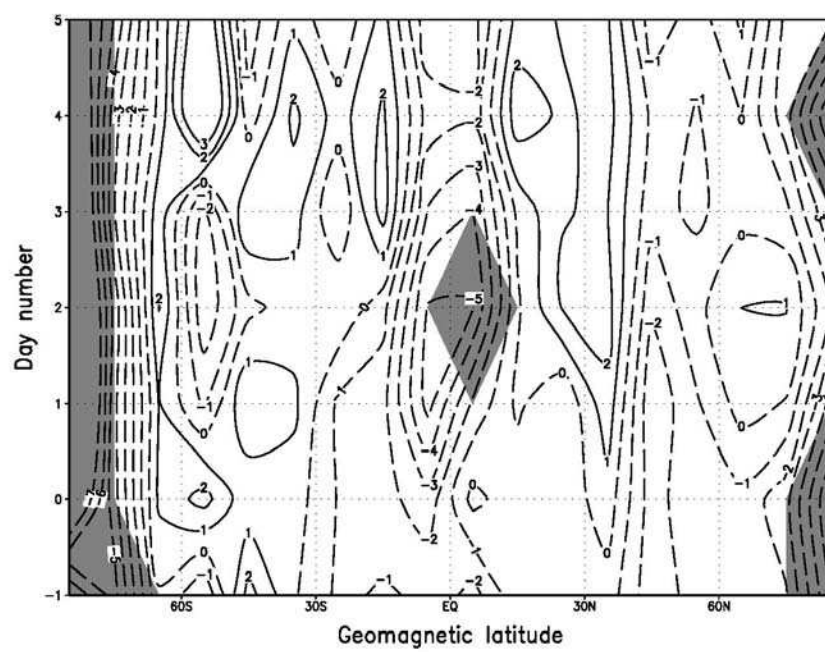


Figure 6b.

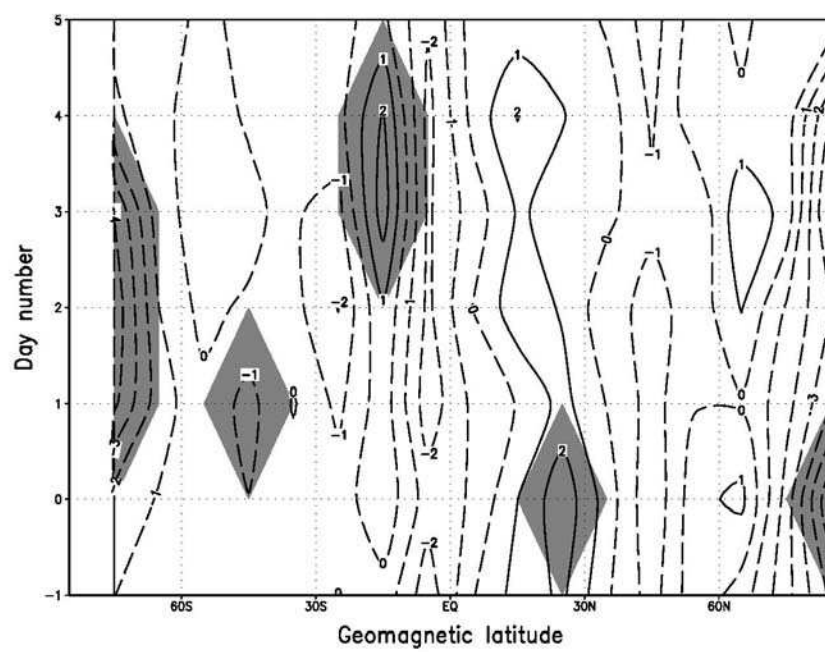


Figure 6c.